An Exploration of the Structural and Bonding Variability in Mixed-Ligand Benzimidazole-2-thione(bromo)(triarylphosphane)dicopper(I) Complexes with Diamond-Shaped $Cu_2(\mu\text{-}X)_2$ Core Structures

Sotiris K. Hadjikakou,*[a] Constantinos D. Antoniadis,[a] Paraskevas Aslanidis,[b] Philip J. Cox,[c] and Athanassios C. Tsipis*[a]

Keywords: Bridging ligands / Copper / Density functional calculations / S ligands

Reaction of copper(I) bromide with benz-1,3-imidazole-2-thione ($bzimtH_2$) in the presence of one equivalent of triphenylphosphane (PPh_3), tri-*meta*-tolylphosphane (tmtp) or tri-*para*-tolylphosphane (tptp) in acetonitrile/methanol solvent afforded dinuclear complexes formulated as $[CuBr(bzimtH_2)(PR_3)]_2$. The new complexes were characterized by IR, UV/Vis, and ^1H NMR spectroscopy, while the crystal structures of $[\{CuBr(\mu_2\text{-}S\text{-}bzimtH_2)(PPh_3)\}_2]_{0.78}[\{Cu(\mu_2\text{-}Br)(PPh_3)(bzimtH_2)\}_2]_{0.22}$ (**1**), $[CuBr(\mu_2\text{-}S\text{-}bzimtH_2)(tmtp)]_2$ (**2**) and $[CuBr(\mu_2\text{-}S\text{-}bzimtH_2)(tptp)]_2$ (**3**) were determined by single-crystal X-ray diffraction methods. In complex **1**, with spectator PPh_3 ligands, the unit cell of the crystal consists of two different half-molecules, both corresponding to the formula $[CuBr(bzimtH_2)(PPh_3)]_2$. One of the two molecules (molecule **A**) is a symmetrical dicopper(I) complex in which the exocyclic thione S-atoms serve as bridges between the Cu^I ions. The second one (molecule **B**) is disordered and can be resolved into two separate entities, one μ_2-S dicopper(I) complex, similar to molecule **A** (molecule **B1**), and another one (molecule **B2**) involving μ_2-Br bridges. In contrast, in complexes **2** and **3**, with spectator tmtp and tptp ligands, only the $bzimtH_2$-bridged dicopper complexes are formed. Density functional calculations at the B3LYP level of theory provided a satisfactory description of the structural, bonding, electronic and related properties of all dicopper complexes exhibiting the "diamond-shaped" $Cu_2(\mu\text{-}X)_2$ (X = S or Br) core structures and account well for their structural preferences.

Introduction

Polynuclear metal–sulfur coordination sites formed by metal ions with a d^{10} configuration constitute the active sites in a super-family of ubiquitous cysteine-rich, low-molecular-weight proteins or polypeptides called metallothioneins.[1,2] Investigations directed to explore the structure and chemistry of metallothioneins in detail are extremely important taking into account that nature makes use of them as multipurpose proteins. Considering that obtaining precise structural information on metallothioneins is a very difficult task, it appears to be appropriate to study the coordination behavior of copper in model complexes reaching from mononuclear to higher nuclearities. All of them might act as structural and spectroscopic models for copper thioneins and might contribute to the understanding of the thionein structure and function. The most useful ligands for modeling cysteine bonding are undoubtedly thiolates. Heterocyclic thiones are an important class of such ligands, and therefore their coordination properties with many transition metals have been studied extensively. Although the coordination chemistry of heterocyclic thiones is characterized by a wealth of coordinating possibilities, studies on their coordination with copper(I) metal centers have revealed that monodentate coordination through the exocyclic thione sulfur atom is the preferred bonding mode of the ligands. Within this class of coordination compounds, the tendency of heterocyclic thiones to bridge metal centers to form oligo- or polymeric species is also well established.[3] In the oligonuclear complexes, which are normally prepared from Cu^I or Cu^{II} salts and thiolates under various reaction conditions in a variety of solvents, the ligands are normally bridging. In the course of our research on the coordination chemistry of copper(I) halides with a variety of thiones and tertiary arylphosphanes we have reported the synthesis and structural studies of symmetrical binuclear species, with the thione ligand coordinated through the exocyclic sulfur atom in a μ_2-S bridging mode.[4–6] However, in many other cases the reaction of copper(I) halides with thione ligands yielded dicopper(I) complexes with a "diamond-shaped" $Cu_2(\mu\text{-}X)_2$ core structure involving the halide as bridging ligands, particularly for the "soft" iodide rather than the "hard" chloride ligand.[4,7]

[a] Section of Inorganic and Analytical Chemistry, Department of Chemistry, University of Ioannina, 45110 Ioannina, Greece
[b] Aristotle University of Thessaloniki, Faculty of Chemistry, Inorganic Chemistry Laboratory, P. O. Box 135, 54124 Thessaloniki, Greece
[c] School of Pharmacy, The Robert Gordon University, Schoolhill, Aberdeen AB10 1FR, Scotland

Thus, the coordination behavior (terminal or bridging) of the thione and halide ligands seems to be determined primarily by the choice of the halide ligand, although the nature of the thione and, to a lesser extent, of the spectator phosphane ligand might also play a significant role. In order to further investigate trends in the formation of these two different types of binuclear copper(I) halide complexes of the general formula $[CuX(thione)(PR_3)]_2$ involving either a double halide or a double thione-sulfur bridge, we report in this work the results of a detailed experimental and quantum chemical (DFT) study of three new, mixed-ligand dinuclear complexes of copper(I) with bromide, benz-1,3-imidazole-2-thione ($bzimtH_2$) and triphenylphosphane (PPh_3), tri-*m*-tolylphosphane (tmtp) or tri-*p*-tolylphosphane (tptp) as ligands pursuing a threefold objective: (i) the examination of the preferred μ_2-S or μ_2-Br bridging mode; (ii) the exploration of the role played by the spectator phosphane ligands, which exert different steric effects while they differ slightly in their basicity; and (iii) the understanding of the role of the bromide ligands, which have a donor capacity on the border between "soft" and "hard", in forming either μ_2-S or μ_2-Br bridges in the dicopper(I) complexes.

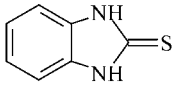

$bzimtH_2$

Results and Discussion

Synthesis

The reaction of equimolar quantities of copper(I) bromide and triphenylphosphane, tri-*m*-tolylphosphane or tri-*p*-tolylphosphane followed by the addition of one equivalent of 1,3-benzimidazole-2-thione ($bzimtH_2$) in dry acetonitrile/methanol solution at 25 °C afforded pale-yellow microcrystalline solids which, on analysis and spectroscopic measurements (IR, ^1H NMR), were found to correspond to the formulae $[\{CuBr(\mu_2\text{-S-}bzimtH_2)(PPh_3)\}_2]_{0.78}[\{Cu(\mu_2\text{-Br})(PPh_3)(bzimtH_2)\}_2]_{0.22}$ (**1**), $[CuBr(\mu_2\text{-S-}bzimtH_2)(tmtp)]_2$ (**2**) and $[CuBr(\mu_2\text{-S-}bzimtH_2)(tptp)]_2$ (**3**). Compounds **1**–**3** are air-stable, diamagnetic, crystalline materials that are soluble in polar solvents such as acetonitrile and dimethyl sulfoxide, slightly soluble in chloroform and dichloromethane, and insoluble in water, diethyl ether and tetrahydrofuran.

The infrared spectra recorded in the range of 4000–250 cm^{-1} show distinct strong vibrational bands due to the phosphane ligand, which remain practically unshifted upon coordination to the metal center. Moreover, the spectra of **1**–**3** contain the usual four "thioamide bands" required by the presence of the heterocyclic thione ligand, as well as the characteristic ν(NH) stretching vibration observed at about 3220 cm^{-1}. The observed shifts of these bands enforced by coordination, in conjunction with the lack of the ν(SH) stretching vibration band, signifies the exclusive S-coordination mode of the 1,3-benzimidazole-2-thione ligand.

The ^1H NMR spectra, recorded in $CDCl_3$, are dominated by the presence of multiplets in the region of δ = 7.45–7.03 ppm attributed to the phenyl protons of the phosphane ligands as well as to the aromatic protons of the thione ligand. The extent of overlapping does not allow resolution between these signals, making assignment of the splitting pattern for the individual thione resonances very difficult. Upon coordination, the methyl protons of the tri-*p*-tolyl- and tri-*m*-tolylphosphane ligands are shifted slightly upfield by 0.09 and 0.08 ppm respectively. Furthermore, the observation of a broad singlet at around δ = 11 ppm due to the proton resonance of the NH groups, and the absence of a signal due to the proton resonance of the SH moiety, strongly suggest that the thione ligand is coordinated to the metal center in its thionato form.

It is well known that deviation from the common four-coordination in copper(I) complexes can be induced by an increase of the bulkiness of the ligands. In this context, according to our previous experience with the use of triarylphosphanes in mixed-ligand Cu^I halide complexes, triphenylphosphane as well as tri-*m*-tolyl- and tri-*p*-tolylphosphane turned out to be relatively small; a coordination number of three could be achieved only for the bulkier tri-*o*-tolylphosphane.[8,9] Similarly, the steric requirements of the neutral heterocyclic thiones used do not affect the coordination number of the complexes, since terminal or bridging S-coordination has been observed but always around a tetrahedrally coordinated copper atom. Thus, on the basis of the chemical composition of the new compounds, we assumed that complexes **1**, **2** and **3** are doubly bridged (μ_2) binuclear complexes. In order to verify our assumption and to confirm the nature of the bridge, we determined the structures of the three complexes by single-crystal X-ray diffraction methods.

Description of the Structures

$[\{CuBr(\mu_2\text{-S-}bzimtH_2)(PPh_3)\}_2]_{0.78}[\{Cu(\mu_2\text{-Br})(PPh_3)(bzimtH_2)\}_2]_{0.22}$ (1)

The unit cell of the crystal consists of two different half-molecules, both corresponding to the formula $[CuBr(bzimtH_2)(PPh_3)]_2$. One of the two molecules (molecule **A**, Figure 1) is a symmetrical dicopper(I) complex in which the thione S-atoms serve as bridges between the Cu^I ions. The second one (molecule **B**, Figure 2) is disordered and can be resolved into two separate entities, one μ_2-S dicopper(I) complex, similar to molecule **A** (molecule **B1**), and another one (molecule **B2**) involving μ_2-Br bridges. The disordered atoms are Br(2), (Br2′), (S2), (S2′), N(4), N(4′), H(4), (H4′), C(26) and (C26′), while the other atoms are considered to overlap. Due to this disorder the hydrogen atoms attached to N(3), C(28) and C(32) in molecule **B** were omitted from the calculations. The six-membered ring C(27)–C(32) has high displacement parameters due to the disorder. Selected bond lengths and angles for **1** are given in Table 1 and ORTEP views showing the atom numbering schemes of molecules **A**, **B1** and **B2** are given in Figures 1

and 2. Molecule **B1** consists of the atoms Cu(2), Br(2), P(2), S(2), N(3), N(4) and C(26)–C(50) (unprimed, 56% occupancy), while the atoms Cu(2), Br(2′), P(2), S(2′), N(3), N(4′), C(26′), C(27)–C(50) (primed, 44% occupancy) belong to the Br-bridged molecule **B2**. The basic structural unit of molecules **A** and **B1** corresponds to a "diamond-shaped" $Cu_2(\mu\text{-}S)_2$ core formed by the operation of an inversion center. The doubly bridging S atoms and the Cu^I metal centers constitute a strictly planar Cu_2S_2 core in which each copper(I) center displays a distorted tetrahedral environment, with the other two positions of the tetrahedra being occupied by a P donor atom of the PPh_3 ligand and a bromide ligand. The two bromide ligands in *trans* positions stabilize the complex further through the formation of two short, symmetrical, intramolecular hydrogen bonds

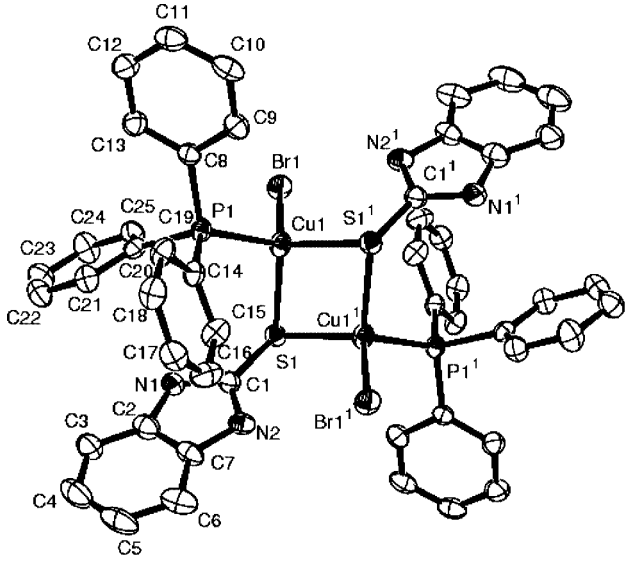

Figure 1. ORTEP view showing the metal environment and the atom labelling scheme in compound **1** (Molecule **A**). Displacement ellipsoids are shown at the 50% probability level.

(Table 1). In general, there are small but definite differences in bond lengths and angles within the central cores of molecules **A** and **B1**. In both structures the bridging sulfur atoms and the two copper atoms form a parallelogram with two short and two longer Cu–S bonds. Although each of these two individual Cu–S distances is not far from the values in other copper(I) complexes with equivalent bonds, the asymmetry in the bridging Cu–S distances is the largest among the thione-S coordinated copper(I) complexes structurally characterized by us so far.

The Cu–P bond lengths in the three individual molecules lie in the range normally found in analogous dicopper(I) complexes with halide or sulfur bridging ligands. In contrast, the significant differences in the corresponding Cu–Br bond lengths are noteworthy. In general terms, the bridging Cu–Br distances are somewhat longer than those found previously in other mixed-ligand dicopper(I) complexes containing bromide, phosphane and heterocyclic thione ligands, but are shorter than those found in $[CuBr(tzdtH)(tmtp)]_2$.[5]

In all three structures the interbond angles around the central copper(I) atoms show remarkable deviations from idealized tetrahedral geometry, with the Br(1)–Cu(1)–S(1) bond angle of 93.89(5)° in molecule **A** representing the most significant distortion. Finally, the S–Cu–S (Br–Cu–Br) and Cu–S–Cu (Cu–Br–Cu) bond angles in the "diamond-shaped" Cu_2S_2 (or Cu_2Br_2) cores are close to the calculated ideal values (109.5 and 70.5°) for a symmetric dimer.

$[CuBr(\mu_2\text{-}S\text{-}bzimtH_2)(tmtp)]_2$ (2) and $[CuBr(\mu_2\text{-}S\text{-}bzimtH_2)(tptp)]_2$ (3)

Selected bond lengths and angles for compounds **2** and **3** are given in Tables 2 and 3 and the molecular structures are displayed in Figures 3 and 4, respectively.

The basic structural unit of both complexes is a dicopper(I) unit with the two copper(I) atoms doubly bridged by two S atoms of the thione ligands to form a strictly planar,

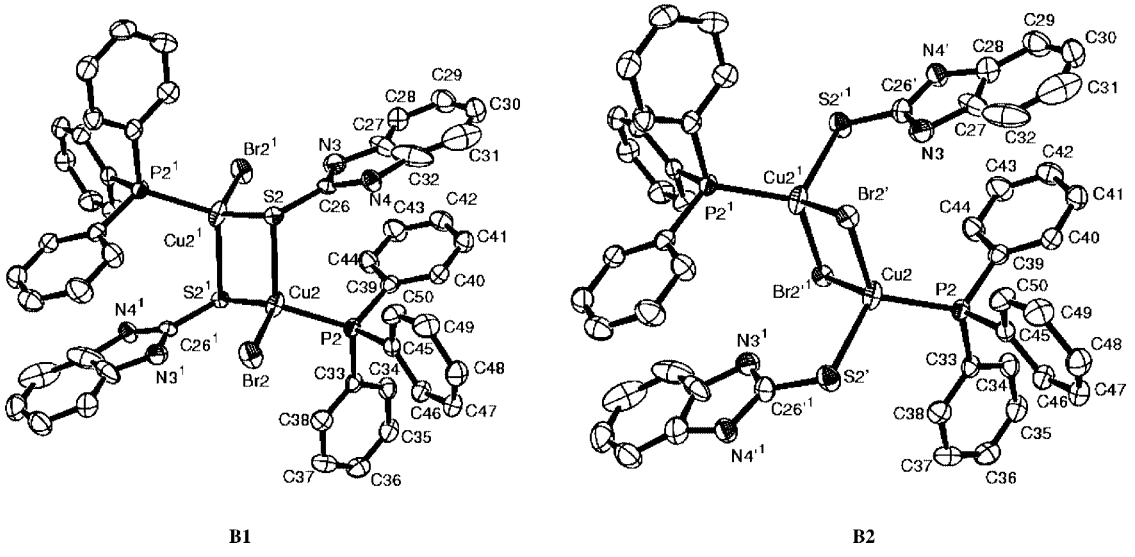

Figure 2. ORTEP views showing the metal environment and the atom labelling scheme in molecules **B1** and **B2**. Displacement ellipsoids are shown at the 50% probability level.

Table 1. Selected bond lengths [Å] and angles [°] for **1**.[a]

Cu(1)–S(1)#1	2.3385(18)	Cu(2)–Br(2′)	2.453(3)
Cu(1)–Br(1)	2.4586(12)	Cu(2)–S(2′)	2.472(4)
Cu(1)–S(1)	2.5330(19)	Cu(2)–Br(2′)#2	2.508(3)
Cu(1)–Cu(1)#1	2.8973(18)	Cu(2)–S(2)	2.535(5)
S(1)–Cu(1)#1	2.3384(18)	Cu(2)–Cu(2)#2	3.0129(18)
P(1)–C(20)	1.822(6)	Br(2′)–Cu(2)#2	2.508(3)
P(1)–C(8)	1.822(6)	S(2)–Cu(2)#2	2.326(5)
P(1)–C(14)	1.827(6)	P(2)–C(39)	1.830(7)
Cu(2)–P(2)	2.2380(19)	P(2)–C(45)	1.832(6)
Cu(2)–S(2)#2	2.326(5)	P(2)–C(33)	1.833(6)
P(1)–Cu(1)–S(1)#1	114.67(7)	Cu(2)–Br(2′)–Cu(2)#2	74.78(8)
S(1)–Cu(1)–S(1)#1	107.13(6)	Br2′)–Cu(2)–S(2′)	101.82(13)
P(1)–Cu(1)–S(1)	112.41(7)	P(2)–Cu(2)–Br(2′)#2	109.42(8)
Br(1)–Cu(1)–S(1)	93.89(5)	Br(2′)–Cu(2)–Br(2′)#2	105.22(8)
Cu(1)#1–S(1)–Cu(1)	72.87(6)	S(2′)–Cu(2)–Br(2′)#2	110.04(14)
P(2)–Cu(2)–S(2)#2	117.48(13)	P(2)–Cu(2)–S(2)	111.20(13)
P(2)–Cu(2)–Br(2)	105.80(6)	S(2)#2–Cu(2)–S(2)	103.52(16)
S(2)#2–Cu(2)–Br(2)	117.57(13)	Br(2)–Cu(2)–S(2)	99.82(12)
P(2)–Cu(2)–Br(2′)	118.11(9)	Cu(2)#2–S(2)–Cu(2)	75.48(16)
P(2)–Cu(2)–S(2′)	111.77(11)		

[a] Symmetry transformations used to generate equivalent atoms: #1: $-x + 2, -y, -z + 1$.

Table 2. Selected bond lengths [Å] and angles [°] for **2**.[a]

Br(1)–Cu(1)	2.5246(4)	S(1)–C(1)	1.709(3)
Cu(1)–P(1)	2.2552(7)	P(1)–C(20)	1.829(2)
Cu(1)–S(1)	2.3681(7)	P(1)–C(8)	1.833(3)
Cu(1)–S(1)#1	2.4507(7)	P(1)–C(14)	1.836(3)
Cu(1)–Cu(1)#1	2.7504(6)		
P(1)–Cu(1)–S(1)#1	113.35(3)	C(1)–S(1)–Cu(1)#1	107.75(8)
S(1)–Cu(1)–S(1)#1	110.42(2)	Cu(1)–S(1)–Cu(1)#1	69.58(2)
P(1)–Cu(1)–Br(1)	108.82(2)	C(20)–P(1)–C(8)	104.40(11)
S(1)–Cu(1)–Br(1)	112.34(2)	C(20)–P(1)–C(14)	103.96(11)
S(1)#1–Cu(1)–Br(1)	93.81(2)	C(8)–P(1)–C(14)	103.97(11)
P(1)–Cu(1)–Cu(1)#1	136.92(3)	C(20)–P(1)–Cu(1)	111.73(8)
S(1)–Cu(1)–Cu(1)#1	56.621(19)	C(8)–P(1)–Cu(1)	119.95(8)
S(1)#1–Cu(1)–Cu(1)#1	53.797(18)	C(14)–P(1)–Cu(1)	111.36(8)
Br(1)–Cu(1)–Cu(1)#1	107.75(8)		

[a] Symmetry transformations used to generate equivalent atoms: #1: $-x + 2, -y, -z + 1$.

Table 3. Selected bond lengths [Å] and angles [°] for **3**.[a]

Br(1)–Cu(1)	2.4734(3)	S(1)–C(1)	1.706(2)
Cu(1)–P(1)	2.2333(6)	P(1)–C(20)	1.817(2)
Cu(1)–S(1)	2.3535(6)	P(1)–C(8)	1.820(2)
Cu(1)–S(1)#1	2.4053(6)	P(1)–C(14)	1.820(2)
Cu(1)–Cu(1)#1	2.8232(5)		
P(1)–Cu(1)–S(1)	107.22 (2)	C(1)–S(1)–Cu(1)	111.66(8)
P(1)–Cu(1)–S(1)#1	117.37(2)	C(1)–S(1)–Cu(1)#1	105.22 (8)
S(1)–Cu(1)–S(1)#1	107.234(19)	Cu(1)–S(1)–Cu(1)#1	72.766(19)
P(1)–Cu(1)–Br(1)	113.174(19)	C(20)–P(1)–C(8)	101.96(10)
S(1)–Cu(1)–Br(1)	112.187(17)	C(20)–P(1)–C(14)	103.20(10)
S(1)#1–Cu(1)–Br(1)	99.532(17)	C(8)–P(1)–C(14)	103.17(10)
P(1)–Cu(1)–Cu(1)#1	129.67(2)	C(20)–P(1)–Cu(1)	116.30(7)
S(1)–Cu(1)–Cu(1)#1	54.463(17)	C(8)–P(1)–Cu(1)	113.46(7)
S(1)#1–Cu(1)–Cu(1)#1	52.771(16)	C(14)–P(1)–Cu(1)	116.81(7)
Br(1)–Cu(1)–Cu(1)#1	117.124(15)		

[a] Symmetry transformations used to generate equivalent atoms: #1: $-x + 1, -y, -z + 1$.

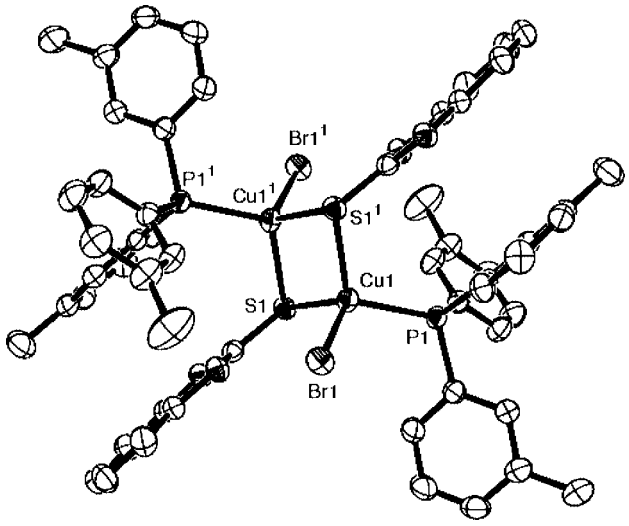

Figure 3. ORTEP view showing the metal environment and the atom labelling scheme in compound **2**. Displacement ellipsoids are shown at the 50% probability level.

four-membered Cu_2S_2 core. The distorted tetrahedral coordination environment around the central copper(I) atoms is completed by one P atom from the phosphane ligand and one bromide ligand. Complex **2** (Figure 3) crystallizes in the monoclinic space group $P2_1/c$ with the unit cell containing two discrete dinuclear species, whereas compound **3** (Figure 4) crystallizes in the triclinic space group $P\bar{1}$. Its structure contains one discrete molecule per unit cell, as well as two CH_3CN, three H_2O and one half CH_3OH lattice molecules; the latter solvate molecules do not interact specifically with the dimer and therefore will not be discussed further.

The Cu–P bond length of 2.2552(7) Å in **2** does not differ significantly from that found in **3** [2.233(6) Å], both values lying in the range normally found for analogous halide- or sulfide-bridged dicopper(I) complexes.[4,7,10] On the other hand, the Cu–Br bonds in **2** and **3** differ remarkably, the latter being shorter by 0.0512 Å. The Cu–Br bond lengths, which are typical for a bromide ligand in the tetrahedral coordination environment of Cu^I complexes, are shorter than those of 2.5693(12) and 2.5369(4) Å found in $[CuBr(dppe)(py2SH)]_2$ [dppe = 1,2-bis(diphenylphosphanyl)ethane][11] and [CuBr(dppb)(pymtH)][12] [dppp = 1,2-bis(diphenylphosphanyl)propane], respectively, but are longer than that found in [CuBr(dppet)(mftztH)].[13] Moreover, both structures exhibit the usual asymmetric $Cu_2(\mu\text{-}S)_2$ core with Cu–S bond lengths in the range found for other dicopper(I) complexes containing bromide, phosphane and heterocyclic thione ligands. Finally, it should be noted that the S–Cu–S and Cu–S–Cu bond angles in the $Cu_2(\mu\text{-}S)_2$

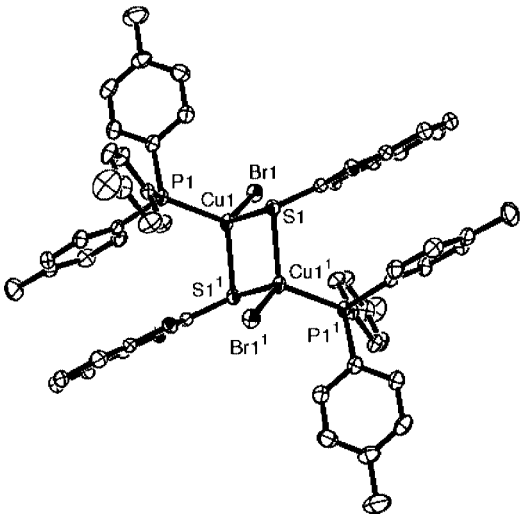

Figure 4. ORTEP view showing the metal environment and the atom labelling scheme in compound **3**. Displacement ellipsoids are shown at the 50% probability level.

core of **2** and **3** closely resemble those of an ideal symmetric dimer.

Electronic Structure Calculations

The structural properties, such as geometrical data, as well as the energetic and spectroscopic properties of the model dicopper complexes $[CuBr(PH_3)(\mu\text{-}S)(imtH_2)]_2$ (**4**) and $[Cu(PH_3)(\mu\text{-}Br)(imtH_2)]_2$ (**5**), which exhibit "diamond-shaped" $Cu_2(\mu\text{-}X)_2$ (X = S or Br) core structures, were examined by electronic structure calculation methods. In order to obtain reliable data it is of outmost importance to find a method/basis set combination that allows the accurate description of the molecules studied herein. In a first attempt, we therefore employed DFT computational techniques at the B3LYP level of theory using a variety of basis sets to reproduce the structure of the $Cu_2(\mu\text{-}X)_2$ (X = S or Br) core of the "real" complexes, the main focus being on the structural parameters of the $Cu_2(\mu\text{-}X)_2$ core in **4** and **5**. The results are compiled in the Supporting Information (Table S1). In all cases the basic structural features of the model compounds **4** and **5** were satisfactorily reproduced by taking into account the different electronic and steric effects of the ligands used to represent the ligands in the "real" complexes. In general terms, the best estimate of the energetic data is that obtained using the larger TZVP and 6-31G(d,p) basis sets. However, more reliable structural data (overall closer to the experiment) were obtained using the DZVP and TZVP rather than the 6-31G(d,p) basis sets. Interestingly, even the smaller SDD basis set performs well with respect to the structural parameters of the model compounds, but could not provide meaningful energetic data. Note that a reliable structure is indispensable for the evaluation of the relative stability of the isomeric species.

Equilibrium Geometries of the Model Compounds

The equilibrium structures of $[CuBr(PH_3)(\mu\text{-}S)(imtH_2)]_2$ (**4**) and $[Cu(PH_3)(\mu\text{-}Br)(imtH_2)]_2$ (**5**) and their monomeric species $[CuBr(PH_3)(imtH_2)]$ (**6**), along with selected structural parameters, computed at the B3LYP/DZVP level of theory are depicted schematically in Figure 5.

Searching the potential energy surface (PES) of the monomeric species $[CuBr(PH_3)(imtH_2)]$ (**6**) we located two stationary points corresponding to two rotamers involving the bromide ligand in a *syn* (**6a**) and *anti* (**6b**) configuration with respect to the imidazole ring. The *syn* rotamer corresponds to the global minimum, while the *anti* one is a local minimum that is 14.7 kcal mol^{-1} higher in energy. The *syn* (**6a**) → *anti* (**6b**) isomerization proceeds across a barrier of 15.1 kcal mol^{-1} through a product-like transition structure $\mathbf{TS_{6a\rightarrow 6b}}$ (Figure 5) with a P–Cu–S–C torsion angle of 57.2°, while the dominant motion of the vibrational mode corresponding to the imaginary frequency (ν_i = 24 cm^{-1}) involves the rotation around the Cu–S bond. Note that the *syn* rotamer is stabilized by the formation of an N–H···Br hydrogen bond. Both rotamers adopt a trigonal planar stereochemistry of C_s symmetry, with the central copper(I) atom and the three donor atoms being coplanar with the imidazole ring. The bending coordination mode of the thione ligand with the Cu^I central atom is noteworthy; the Cu^I–S–C bond angles are 104.3° and 107.6° in the *syn* and *anti* rotamers, respectively. The bending coordination mode of the thione ligand is that expected on the grounds of the bonding interactions between the Cu^I and thione ligand orbitals, which will be discussed later on.

The equilibrium geometries of the dimeric species $[CuBr(PH_3)(\mu\text{-}S)(imtH_2)]_2$ (**4**) and $[CuS(PH_3)(\mu\text{-}Br)(imtH_2)]_2$ (**5**) correspond to a "diamond-shaped" $Cu_2(\mu\text{-}X)_2$ (X = S or Br) core structure where the copper(I) atoms display a distorted tetrahedral coordination environment. The $Cu_2(\mu\text{-}X)_2Cu$ (X = S or Br) parallelogram is perfectly planar with two long and two short asymmetric Cu–X bonds, in line with the available X-ray crystal structure data. The asymmetry in the Cu–X bond lengths of the $Cu_2(\mu\text{-}X)_2Cu$ parallelogram is more pronounced for X = S rather than for X = Br, the difference in the Cu–X bond lengths being 8.4 and 4.5 pm, respectively. The intermetallic Cu···Cu distance is 322.3 and 316.0 pm for the μ_2-S and μ_2-Br dimers, respectively. On the other hand, the X···X distance is equal to 384.9 and 416.2 pm for **4** and **5**, respectively. No cross-ring interactions are possible in either **4** or **5** due to the long Cu···Cu or X···X distances, in agreement with the framework-electron counting (FEC) rule introduced by Alvarez et al.[14] to account for the formation or breaking of transannular bonds in dimetal systems that contain a simple "diamond-shaped" $M_2(\mu\text{-}X)_2$ core structure.

At all levels of theory the μ_2-Br-bridged dimer **5** is predicted to be slightly more stable than the μ_2-S-bridged dimer **4** by 2.5–5.4 kcal mol^{-1}. The computed dimerization energy for **4** and **5** was found to be 18.8 and 21.7 kcal mol^{-1}, respectively, at the B3LYP/TZVP level of theory. The dimerization and relative energies of the model complexes **4** and **5** computed at the B3LYP level of theory using a variety of basis sets are given in detail in the Supporting Information (Table S2). The low computed dimerization energy indicates that **4** and **5** correspond to loose associations of the mono-

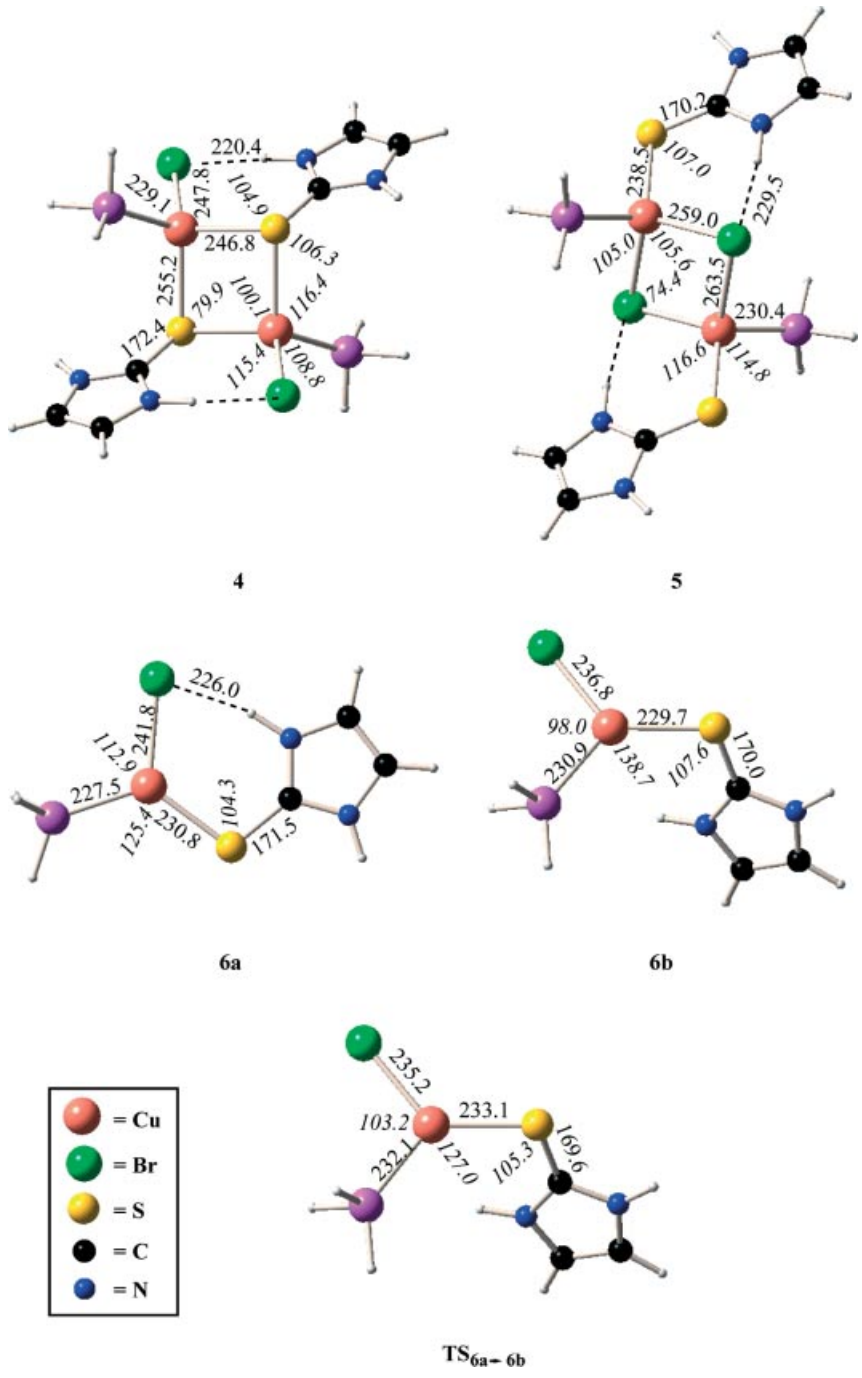

Figure 5. Equilibrium geometries of $[CuBr(PH_3)(\mu\text{-}S)(imtH_2)]_2$ (**4**), $[CuS(PH_3)(\mu\text{-}Br)(imtH_2)]_2$ (**5**) and the monomeric species $[CuBr(PH_3)(imtH_2)]$ in the *syn* (**6a**) and *anti* (**6b**) configurations computed at the B3LYP/DZVP level of theory.

meric species **6a** and strongly suggests that both isomers could be formed during the synthesis. Moreover, because of the low dissociation energy of the dimers they are expected to be in equilibrium with their monomers, therefore the two isomers and their monomeric species could coexist in the solid state, in line with the experiment. The interconversion of the two isomers should follow a dissociative (S_N1) mechanism, as shown in Scheme 1. According to this mechanism the dimer dissociates to the monomer, which then re-associates with a different orientation. The total energies given are those computed at the B3LYP/TZVP level of theory.

Electronic Structure and Bonding Description of the Model Compounds

In order to gain insight into the electronic and bonding properties of the monomer **6** and the dimers **4** and **5** the relevant molecular orbitals (MOs) and the Mulliken population analyses were extracted from the B3LYP/DZVP cal-

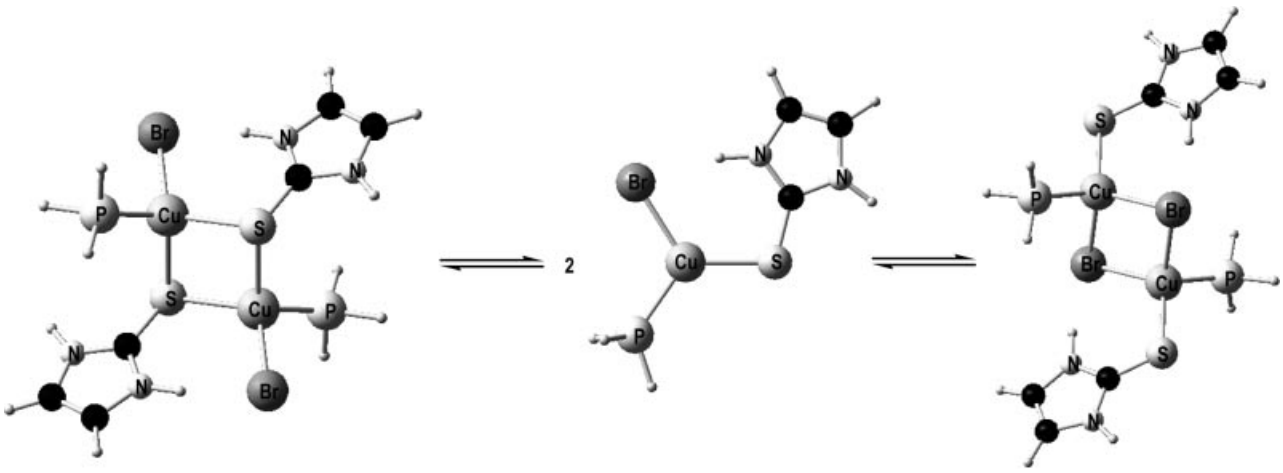

Scheme 1. Mechanism of the **4** → **5** interconversion through a dissociative (S_N1) pathway.

culations. Both the $imtH_2$ and $bzimtH_2$ ligands possess two occupied frontier molecular orbitals (HOMO and HOMO-1) with high sulfur 3p-orbital character (Scheme 2), which are the orbitals primarily involved in the formation of the Cu–S coordination bond. The two π-type MOs were labeled as π_{ip} and π_{op} following the nomenclature previously established by Solomon et al.[15] for phenolate and by Halfen et al.[16] for thiophenolate ligands. The π_{ip} orbital lies in the plane of the imidazole ring, while the π_{op} orbital is perpendicular to this plane. In light of the perfect planarity of the $[CuBr(PH_3)(imtH_2)]$ model compound it is the π_{ip} MO of the thione ligand which participates in the bonding interactions with a vacant metal orbital [a 4s orbital of Cu^I hybridized by mixing with the 4p orbitals in the bent

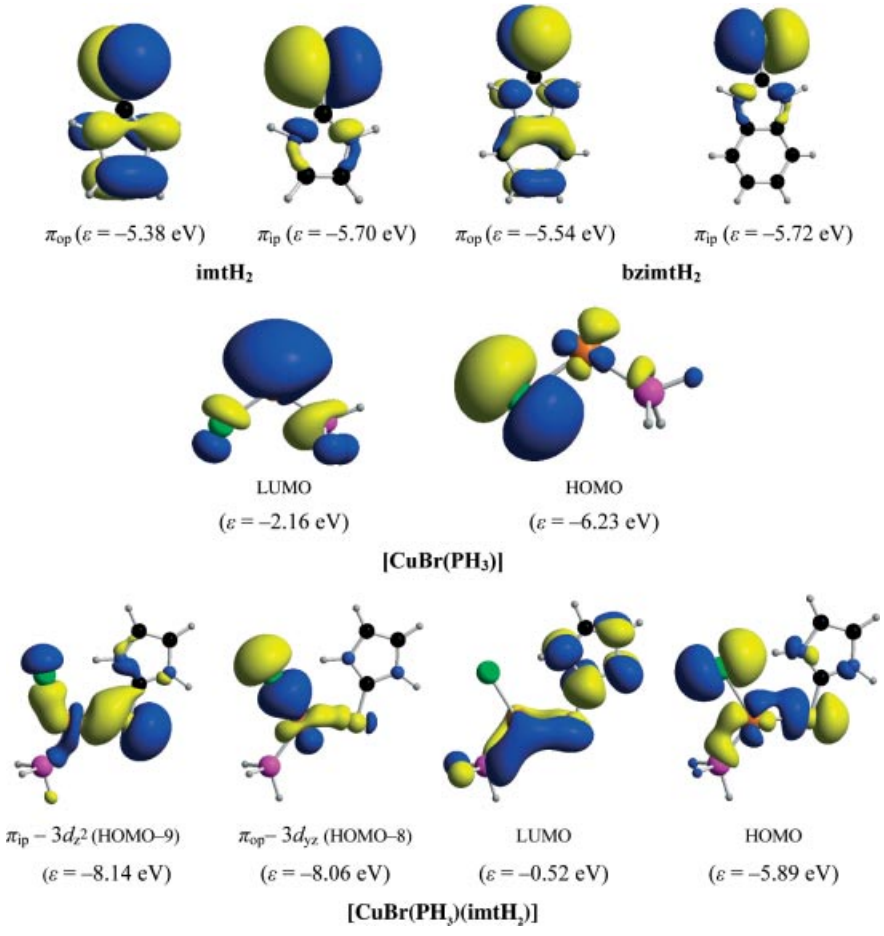

Scheme 2. The most relevant MOs of the $imtH_2$ and $bzimtH_2$ thione ligands and the model $[CuBr(PH_3)]$ and $[CuBr(PH_3)(imtH_2)]$ complexes.

$CuBr(PH_3)$ fragment, the LUMO in Scheme 2] to form the σ Cu^I–S coordination bond. In order to achieve maximum overlap the π_{ip} MO should point primarily along the Cu^I–S bond, which nicely explains the Cu^I–S–C bending (Cu–S–C bond angle of 104.3°). The π_{op} is perpendicular to the Cu^I–S vector and therefore interacts in a π fashion with a vacant metal orbital.

According to the natural bond orbital (NBO) population analysis the bonding σ(Cu–S) interaction between the Cu and S atoms is constructed from an s NAO (93.29% s-character) on a Cu atom interacting with a p NAO (89.36% p-character) on a sulfur atom, and thus has the form $\sigma(Cu\text{–}S) = (0.2868)s_{Cu} + (0.9580)p_S$.

The Mulliken population analysis data given in Table 4 indicate that there is a charge transfer of about 0.14 charge units of electron density from the sulfur donor atom to the central Cu^I atom upon coordination of the thione ligand to the Cu^I metal center of the $[CuBr(PH_3)]$ fragment. This charge transfer increases to 0.20 charge units of electron density upon dimerization of the monomeric species **6**, when sulfur bridges are formed, but remains unchanged when bromide bridges are formed. The charge transfer from sulfur to Cu^I, which is a result of both σ-dative and π-back-bonding interactions, results in the weakening of the C=S bond of the thione ligand, which thus acquires a partial double-bond character that is reflected in the bond overlap population (*bop*) values (Table 4), which correlate well with the charge transferred from S to Cu^I. Moreover, the Cu–S *bop* values indicate that the Cu–S···Cu bridge is not symmetric, while the Cu–S bonds are remarkably weakened upon dimerization.

Based upon the nature of the FMOs of the monomeric species $[CuBr(PH_3)(imtH_2)]$ (**6**; Scheme 2) it can be envisaged that the monomers **6** could be dimerized through favorable HOMO–LUMO interactions that form either weak μ-S or μ-Br bridges. On the other hand, the high HOMO–LUMO energy gap of 5.37 eV illustrates the high stability of the monomer, which should coexist in equilibrium with the dimers. It should be noted that copper is normally monovalent in its thiolate complexes and the coordination is normally trigonal planar, although a number of linearly coordinated examples are known. In oligonuclear complexes, which are normally prepared from Cu^I or Cu^{II} salts and thiolates under various reaction conditions in solvents such as methanol, the ligands are normally bridging. In the series of dinuclear copper thiolates only a few cases are known with a central four-membered Cu_2S_2 unit, probably because of the closed-shell $d^{10}\cdots d^{10}$ Cu···Cu and ligand···ligand repulsions. Examples are $[Cu_2(mimtH)_6]^{2+}$ (mimtH = 1-methylimidazoline-2-thione),[17] the thione complex $[Cu_2\text{-}(SNC_5H_5)_6]Cl_2$,[18] and the thiolate complex $[Cu_2(SC_6H_4\text{-}o\text{-}Me)_2(1,10\text{-phen})_2]$ with phenanthroline as co-ligand.[19]

Single-Point Calculations on the "Real" Complexes

For the single-point calculations, the geometries were based on the corresponding X-ray crystal structures. Moreover, calculations were performed on the monomeric species $[CuBr(PPH_3)(bzimtH_2)]$ (**7**), $[CuBr(tmtp)(bzimtH_2)]$ (**8**) and $[CuBr(tptp)(bzimtH_2)]$ (**9**) resulting from the adiabatic dissociation of the dimers for the dissociation energy to be estimated. The energetic and electronic properties of the "real" complexes and their monomeric species, computed at the B3LYP/DZVP level, are compiled in Table 5.

It can be seen that complex **1A**, which contains μ_2-S bridges, is more stable than its isomeric complex **1B**, which contains μ_2-Br bridges, by about 121 kcal mol^{-1} at the B3LYP/DZVP level. The predicted higher stability of isomer **1A** accounts well for the estimated experimental occupancy of **1A** in the unit cell of the crystal (about 78%). The coexistence of the thermodynamically less stable isomer **1B** in the solid state could be attributed to steric and crystal-packing effects. The dimerization energy of **1A** was predicted to be 52.3 kcal mol^{-1}, thus illustrating that the sulfur bridges are relatively weak. In contrast, the dimerization energy of **1B** was predicted to be only 2.4 kcal mol^{-1}, thus indicating that **1B** corresponds practically to the three-coordinate monomer **7B**. It should be noted that **7B** is stabilized with respect to its isomer **7A** by 35.6 kcal mol^{-1} at the B3LYP/DZVP level. The higher stability of **7B** is also reflected in the higher HOMO–LUMO energy gap (4.37 vs. 3.40 eV). The weak association of the monomer **7B** to form **1B** is also mirrored in the relatively small change of the electron-density distribution introduced by the association of the monomers through the formation of the μ_2-Br bridges.

Finally, complex **2**, which contains the spectator tmtp ligand, is slightly more stable than isomer **3**, which contains

Table 4. Electronic properties of $imtH_2$, $[CuBr(PH_3)(imt)]$, $[CuBr(PH_3)(\mu\text{-}S)(imt)]_2$ and $[CuS(PH_3)(\mu\text{-}Br)(imt)]_2$ model compounds computed at the B3LYP/DZVP level.

	$imtH_2$	$[CuBr(PH_3)(imt)]$	$[CuBr(PH_3)(\mu\text{-}S)(imt)]_2$	$[CuS(PH_3)(\mu\text{-}Br)(imt)]_2$
q_{Cu}		0.04	0.06	0.09
q_S	–0.32	–0.18	–0.12	–0.17
q_{Br}		–0.52	–0.54	–0.46
q_P		–0.05	–0.08	–0.08
bop(Cu1–S)		0.242	0.162	0.181
bop(Cu2–S)			0.102	0.181
bop(Cu1–Br)		0.198	0.160	0.118
bop(Cu2–Br)		0.257	0.160	0.092
bop(Cu–P)		0.128	0.091	0.075
bop(C–S)	0.570	0.393	0.341	0.412

Table 5. Total electronic energies (Hartrees), dissociation energies (*DE*, kcal mol^{-1}), HOMO and LUMO eigenvalues (eV), and Mulliken net atomic charges of the "real" complexes **1**–**3** and their monomeric species, computed at the B3LYP/DZVP level.

	1A	**1B**	**2**	**3**	**7A**	**7B**	**8**	**9**
E_{tot} (Hartrees)	–12056.27403	–12056.08097	–12292.02752	–12292.01458	–6028.09532	–6028.03856	–6146.00358	–6145.97435
DE	52.3	2.4	12.7	41.3	–	–	–	–
ε_{HOMO} (eV)	–4.94	–4.87	–4.91	–4.81	–5.01	–5.50	–5.35	–4.85
ε_{LUMO} (eV)	–1.32	–0.73	–1.22	–1.22	–1.61	–1.13	–1.36	–1.60
q_{Cu}	–0.23	–0.16	–0.22	–0.29	–0.04	–0.08	–0.08	–0.11
q_S	–0.02	–0.22	–0.01	0.01	–0.14	–0.26	–0.17	–0.10
q_{Br}	–0.56	–0.38	–0.60	–0.59	–0.55	–0.49	–0.60	–0.55
q_P	0.67	0.65	0.64	0.68	0.57	0.59	0.56	0.56

tptp, by about 8.2 kcal mol^{-1}. The same holds also true for the corresponding monomeric species. The monomer **8** is more stable than monomer **9** by about 18.3 kcal mol^{-1} at the B3LYP/DZVP level. The dimerization energies for **8** and **9** were predicted to be 12.8 and 41.3 kcal mol^{-1}, respectively.

Concluding Remarks

We have reported the synthesis of a new series of dinuclear copper(I) complexes formulated as [CuBr-(bzimtH$_2$)(PR$_3$)]$_2$ formed by treatment of copper(I) bromide with benz-1,3-imidazole-2-thione (bzimtH$_2$) in the presence of one equivalent of triphenylphosphane (PPh$_3$), tri-*meta*-tolylphosphane (tmtp) or tri-*para*-tolylphosphane (tptp) in acetonitrile/methanol solvent. The crystal structures of the new complexes [{CuBr(μ_2-S-bzimtH$_2$)(PPh$_3$)}$_2$]$_{0.78}$[{Cu-(μ_2-Br) (PPh$_3$)(bzimtH$_2$)}$_2$]$_{0.22}$ (**1**), [CuBr(μ_2-S-bzimtH$_2$)-(tmtp)]$_2$ (**2**) and [CuBr(μ_2-S-bzimtH$_2$)(tptp)]$_2$ (**3**) have been determined by single-crystal X-ray diffraction methods. Depending on the spectator phosphane ligands either μ_2-S- or μ_2-Br-bridged dimers are formed. In some cases the monomeric three-coordinate Cu^I complexes seem to be stable as well. Thus, for the simple PH$_3$ ligand (a strong σ-donor) both dimeric species are predicted to be formed in equal proportions upon treatment of copper(I) bromide with the thione ligand in the presence of PH$_3$. On the other hand, with the PPh$_3$ ligand (a weaker σ-donor and stronger π-acceptor ligand than PH$_3$) the two isomeric forms involving μ_2-S or μ_2-Br bridges coexist in the solid state, with the former being favored (about 78%). In contrast, with the spectator tmtp and tptp ligands (with comparable electronic effects to those of PPh$_3$, but differing significantly in their steric effects) only the μ_2-S-bridged dicopper complexes are formed. Density functional calculations at the B3LYP level of theory provide a satisfactory description of the bonding, electronic and related properties of the "real" and model dicopper complexes exhibiting the "diamond-shaped" Cu$_2$(μ-X)$_2$ (X = S or Br) core structures and account well for their structural preferences. In all complexes the coordination of the thione ligand is further stabilized by Br···H–N bond formation, which is more pronounced in the μ_2-S bridged dimers. No Cu^I···Cu^I interactions are predicted to occur either in the μ_2-S- or μ_2-Br- bridged dicopper complexes.

Experimental Section

Materials and Instruments: Copper(I) bromide, triphenylphosphane, tri-*m*-tolylphosphane, tri-*p*-tolylphosphane and solvents are commercially available and were used as obtained, while benz-1,3-imidazole-2-thione was recrystallized from hot ethanol prior to use. Elemental analyses for C, H and N were carried out with a Carlo Erba EA MODEL 1108. Melting points were measured in open tubes with a STUART scientific apparatus and are uncorrected. IR spectra in the region of 4000–370 cm^{-1} were obtained in KBr discs while far-IR spectra in the region of 400–50 cm^{-1} were obtained in polyethylene discs, with a Perkin–Elmer Spectrum GX FT-IR spectrometer. ^{1}H NMR spectra were recorded on a Bruker 400 MHFT NMR instrument in CDCl$_3$ solutions with chemical shifts given in ppm relative to internal TMS.

Synthesis of the Complexes 1–3: The appropriate phosphane (0.5 mmol) was added to a suspension of copper(I) bromide (71.7 mg, 0.5 mmol) in 30 mL of dry acetonitrile, and the mixture was stirred for 2 h at ambient temperature during which time a white precipitate of [CuBr(PR$_3$)$_n$]$_m$ [PR$_3$ = triphenylphosphane (PPh$_3$), tri-*p*-tolylphosphane (tptp) or tri-*m*-tolylphosphane (tmtp)] formed. A solution of benz-1,3-imidazole-2-thione (75 mg, 0.5 mmol) in 20 mL of methanol was added dropwise to the reaction mixture whereupon the white precipitate gradually disappeared. After stirring at ambient temperature overnight, the resulting clear solution was filtered off and left to evaporate. The microcrystalline solid that deposited upon standing for several days was filtered off and dried in vacuo.

[{CuBr(μ_2-S-bzimtH$_2$)(PPh$_3$)}$_2$]$_{0.78}$[{Cu(μ_2-Br)(PPh$_3$)(bzimtH$_2$)}$_2$]$_{0.22}$ (1): Pale-yellow crystals; m.p. 235–236 °C. $C_{50}H_{42}Br_2Cu_2N_4P_2S_2$: calcd. C 54.01, H 3.81, N 5.04; found C 53.94, H 3.69, N 5.06. IR: $\tilde{\nu}$ = 3217 m, 3052 s, 2969 m, 2852 m, 1619 s, 1500 vs, 1478 m, 1460 vs, 1434 vs, 1390 m, 1361 s, 1346 s, 1258 m, 1216 m, 1174 vs, 1094 s, 744 vs, 598 s, 520 vs, 497 vs cm^{-1}; far-IR: $\tilde{\nu}$ = 279 w, 219 w, 205 w, 200 w, 192 w, 174 s, 161 s, 151 vs, 146 m, 132 w, 127 w, 121 s, 100 w, 89 w, 80 w, 74 w, 57 w, 38 s cm^{-1}. ^{1}H NMR (CDCl$_3$): δ = 10.92 (s, 2 H, NH), 7.47–7.41 + 7.34–7.22 (m, 15 H, PC$_6$H$_5$ + m, 4 H, CH$_{bzimtH2}$) ppm.

[CuBr(μ_2-S-bzimtH$_2$)(tmtp)]$_2$ (2): Pale-yellow crystals; m.p. 285–288 °C. $C_{56}H_{54}Br_2Cu_2N_4P_2S_2$: calcd. C 56.24, H 4.55, N 4.68; found C 55.93, H 4.48, N 4.62. IR: $\tilde{\nu}$ = 3235 m, 3043 m, 2935 w, 1492 s, 1460 vs, 1360 m, 1341 m, 1167 s, 1103 m, 778 s, 746 vs, 695 vs, 598 s, 548 s; 459 m cm^{-1}; far-IR: $\tilde{\nu}$ = 136 w, 121 w, 96 s, 89 m, 80 w, 73 w, 65 w, 57 m, 37 s cm^{-1}. ^{1}H NMR (CDCl$_3$): δ = 11.03 (s, 2 H, NH), 7.31–7.24 + 7.17–7.13 (m, 12 H, PC$_6$H$_5$ + m, 4 H, CH$_{bzimtH2}$), 2.20 (s, 9 H, CH$_3$-C) ppm.

[CuBr(μ_2-S-bzimtH$_2$)(tptp)]$_2$ (3): Pale-yellow crystals; m.p. 225–227 °C; [($C_{56}H_{54}Cu_2Br_2N_4P_2S_2$)·0.5($CH_3OH$)·2($CH_3CN$)·3($H_2O$)]:

calcd. C 53.08, H 5.14, N 6.35; found C 52.90, H 5.08, N 6.26. IR: 3220 m, 3071 s, 2976 w, 2863 w, 1620 s, 1597 s, 1498 vs, 1465 vs, 1396 s, 1360 s, 1277 m, 1217 m, 1187 vs, 1097 vs, 1018 s, 807 vs, 745 vs, 709 s, 641 s, 630 s, 600 s, 518 vs, 418 vs cm^{-1}; far-IR: $\tilde{\nu}$ = 144 w, 127 w, 113 w, 104 w, 95 s, 81 m, 57 s, 37 s cm^{-1}. ^1H NMR ($CDCl_3$): δ = 11.09 (s, 2H, NH), 7.36–7.31 + 7.27–7.03 (m, 12 H, PC_6H_5 + m, 4 H, $CH_{bzimtH2}$), 2.23 (s, 9 H, CH_3-C) ppm.

X-ray Structural Determinations: Single crystals suitable for crystal structure analysis were obtained by slow evaporation of acetonitrile/methanol solutions of the complexes at room temperature. X-ray diffraction data were collected on a Bruker-Nonius Kappa CCD area-detector diffractometer. The programs DENZO[20] and COLLECT[21] were used in data collection and cell refinement. Details of crystal and structure refinement are shown in Table 6. The structures were solved with SIR97[22] and refined with SHELX-97.[23] Molecular plots were obtained with ORTEP-3.[24]
CCDC-241984 (**1**), -241985 (**2**) and -241986 (**3**) contain the supplementary crystallographic data for this paper. These data can be obtained free of charge from The Cambridge Crystallographic Data Centre via www.ccdc.cam.ac.uk/data_request/cif.

Computational Details: The structural, electronic and energetic properties of all compounds were computed with Becke's three-parameter hybrid functional[25,26] combined with the Lee–Yang–Parr[27] correlation functional (B3LYP level of density functional theory) using several basis sets, such as the SDD basis set, which describes valence electrons with an [8s,7p,6d/6s,5p,3d] valence basis set and Stuttgart–Dresden relativistic ECPs;[28] the larger all-electron double-zeta (DZVP) basis set;[29] the split-valence 6-31G(d) basis set; the LANL2DZ basis set, which describes valence electrons with a [5s,6p,4d/3s,3p,2d] valence basis set and Los Alamos ECPs;[30–32] the LANL2DZ basis set for copper combined with the 6-31G(d) basis for the non-metal atoms. The hybrid B3LYP functional was used since it gives acceptable results for molecular energies and geometries, as well as proton donation, and weak and strong H-bonds.[33–38] No constraints were imposed on the geometry. Full geometry optimization was performed for each structure using Schlegel's analytical gradient method,[39] and the attainment of the energy minimum was verified by calculating the vibrational frequencies that result in an absence of imaginary eigenvalues. All the stationary points were identified for minima (number of imaginary frequencies NIMAG = 0) or transition states (NIMAG = 1). All calculations were performed using the GAUSSIAN 03 series of programs.[40] Moreover, the qualitative concepts and the graphs derived from the Chem3D program suite[41] highlight the basic interactions found from the DFT calculations. Because of the computational cost due to the relatively big size of the compounds under consideration, to obtain a computationally convenient size we used

Table 6. Crystal data and structure refinement for $[\{CuBr(\mu_2\text{-S-bzimtH}_2)(PPh_3)\}_2]_{0.78}[\{Cu(\mu_2\text{-Br})(PPh_3)(bzimtH_2)\}_2]_{0.22}$ (**1**), $[CuBr(\mu_2\text{-S-bzimtH}_2)(tmtp)]_2$ (**2**) and $[CuBr(\mu_2\text{-S-bzimtH}_2)(tptp)]_2$ (**3**).

	1	**2**	**3**
Chemical formula	$C_{50}H_{42}Br_2Cu_2N_4P_2S_2$	$C_{56}H_{54}Br_2Cu_2N_4P_2S_2$	$[C_{28}H_{27}BrCuN_2PS]_2{\cdot}2CH_3CN{\cdot}3H_2O{\cdot}0.5CH_3OH$
Formula weight	1111.84	598.00	1347.56
Temperature	150(2) K	120(2) K	120(2) K
Wavelength	0.71073 Å	0.71073 Å	0.71073 Å
Crystal system	triclinic	monoclinic	triclinic
Space group	$P\bar{1}$	$P2_1/c$	$P\bar{1}$
Unit cell dimensions	a = 12.429(5) Å	a = 13.7360(3) Å	a = 10.3831(3) Å
	b = 13.641(5) Å	b = 15.6560(4) Å	b = 12.0888(3) Å
	c = 14.200(5) Å	c = 12.6520(3) Å	c = 13.4736(4) Å
	α = 94.823(5)°	α = 90°	α = 76.8516(15)°
	β = 90.552(5)°	β = 103.0553(14)°	β = 82.8213(13)°
	γ = 103.806(5)°	γ = 90°	γ = 72.6689(15)°
Volume	2328.6(15) $Å^3$	2650.50(11) $Å^3$	1569.11(8) $Å^3$
Z	2	2	1
Density (calculated)	1.586 $Mg\,m^{-3}$	1.499 $Mg\,m^{-3}$	1.427 $Mg\,m^{-3}$
Absorption coefficient	2.828 mm^{-1}	2.490 mm^{-1}	2.118 mm^{-1}
F_{000}	1120	1216	691
Crystal size	0.10 × 0.10 × 0.05 mm	0.40 × 0.20 × 0.18 mm	0.33 × 0.28 × 0.12 mm
Theta range for data collection	3.02 to 26.41°	3.01 to 27.48°	3.06 to 27.75°
Index ranges	$-15 \le h \le 15$	$-15 \le h \le 17$	$-13 \le h \le 13$
	$-17 \le k \le 17$	$-20 \le k \le 20$	$-15 \le k \le 15$
	$-16 \le l \le 17$	$-16 \le l \le 16$	$-17 \le l \le 17$
Reflections collected	37 573	2 0305	13 558
Independent reflections	9508 [R(int) = 0.0736]	5923 [R(int) = 0.0519]	7196 [R(int) = 0.0350]
Completeness to theta	99.4% (for theta = 26.41°)	97.4% (for theta = 27.48°)	97.1% (for theta = 27.75°)
Max. and min. transmission	0.8715 and 0.7652	0.6628 and 0.4358	0.7852 and 0.5416
Refinement method	Full-matrix least squares on F^2	Full-matrix least squares on F^2	Full-matrix least squares on F^2
Data/restrains/parameters	7518/0/597	5923/0/310	7196/4/379
Goodness-of-fit on F^2 (S)	1.124	1.053	1.043
Final R indices [$I > 2\sigma(I)$]	$R1$ = 0.0675, $wR2$ = 0.1638	$R1$ = 0.0353, $wR2$ = 0.0740	$R1$ = 0.0344, $wR2$ = 0.0786
R indices (all data)	$R1$ = 0.0869, $wR2$ = 0.1722	$R1$ = 0.0475, $wR2$ = 0.0793	$R1$ = 0.0525, $wR2$ = 0.0846
Final weighting scheme	[a]	[b]	[c]
Largest diff. peak and hole	1.585 and –0.834 e $Å^{-3}$	0.334 and –0.464 e $Å^{-3}$	0.367 and –0.522 e $Å^{-3}$

[a] Calcd. $w = 1/[\sigma^2(F_o^2) + (0.0381P)^2 + 18.6558P]$ where $P = (F_o^2 + 2F_c^2)/3$. [b] Calcd. $w = 1/[\sigma^2(F_o^2) + (0.0218P)^2 + 2.0748P]$ where $P = (F_o^2 + 2F_c^2)/3$. [c] Calcd. $w = 1/[\sigma^2(F_o^2) + (0.0416P)^2 + 0.0506P]$ where $P = (F_o^2 + 2F_c^2)/3$.

models resulting from substitution of the phenyl groups of the spectator phosphane ligands by H atoms, while the benzimidazole-2-thione was replaced by the imidazole-2-thione ($imtH_2$) ligand. The use of such models does not alter the description of the "core" region of the compounds and is ultimately the most efficient and productive route for modeling the electronic structure and related properties of relatively large transition metal coordination compounds. Single point energy calculations on the "real" dicopper(I) complexes were also performed at the B3LYP/LANL2DZ level using the X-ray structural parameters of the two isomeric forms that coexist in the solid state.

[1] P. Gonzalez-Duarte, in *Comprehensive Coordination Chemistry II, Vol. 8* (Eds.: J. A. McLeverty, T. J. Meyer), Elsevier, Amsterdam, **2004**, pp. 213.
[2] G. Henkel, B. Krebs, *Chem. Rev.* **2004**, *104*, 801.
[3] S. E. Raper, *Coord. Chem. Rev.* **1994**, *129*, 91.
[4] S. K. Hadjikakou, P. Aslanidis, P. D. Akrivos, P. Karagiannidis, B. Kojic-Prodic, M. Luic, *Inorg. Chim. Acta* **1992**, *197*, 31.
[5] P. Aslanidis, S. K. Hadjikakou, P. Karagiannidis, B. Kojic-Prodic, M. Luic, *Polyhedron* **1994**, *13*, 3119.
[6] P. Aslanidis, P. J. Cox, S. K. Hadjikakou, C. D. Antoniadis, *Eur. J. Inorg. Chem.* **2002**, 2216.
[7] S. K. Hadjikakou, P. Aslanidis, P. Karagiannidis, A. Hountas, A. Terzis, *Inorg. Chim. Acta* **1991**, *184*, 161.
[8] S. K. Hadjikakou, P. Aslanidis, P. Karagiannidis, A. Hountas, A. Terzis, *Inorg. Chim. Acta* **1991**, *186*, 199.
[9] S. K. Hadjikakou, P. Aslanidis, P. Karagiannidis, A. Aubry, S. Skoulika, *Inorg. Chim. Acta* **1992**, *193*, 129.
[10] P. Karagiannidis, S. K. Hadjikakou, P. Aslanidis, A. Hountas, *Inorg. Chim. Acta* **1990**, *178*, 27.
[11] P. J. Cox, P. Aslanidis, P. Karagiannidis, *Polyhedron* **2000**, *19*, 1615.
[12] P. Aslanidis, P. J. Cox, S. Divanidis, A. C. Tsipis, *Inorg. Chem.* **2002**, *41*, 6875.
[13] P. Aslanidis, P. J. Cox, S. Divanidis, P. Karagiannidis, *Inorg. Chim. Acta* **2004**, *357*, 1063.
[14] S. Alvarez, A. A. Palacios, G. Aullon, *Coord. Chem. Rev.* **1999**, *185–186*, 431 and references cited therein.
[15] M. I. Davis, A. M. Orville, F. Neese, J. M. Zaleski, J. D. Lipscomb, E. I. Solomon, *J. Am. Chem. Soc.* **2002**, *124*, 602.
[16] D. C. Fox, A. T. Fiedler, H. L. Halfen, T. C. Brunold, J. A. Halfen, *J. Am. Chem. Soc.* **2004**, *126*, 7627.
[17] E. S. Raper, J. R. Creighton, D. Robson, J. D. Wilson, W. Clegg, A. Milne, *Inorg. Chim. Acta* **1988**, *143*, 95.
[18] E. C. Constable, P. R. Raithby, *J. Chem. Soc., Dalton Trans.* **1987**, 2281.
[19] R. K. Chadha, R. Kumar, D. G. Tuck, *Can. J. Chem.* **1987**, *65*, 1336.
[20] Z. Otwinowski, W. Minor, in *Methods in Enzymology, Vol. 276, Part A* (Eds.: C. W. Carter, Jr, R. M. Sweet), Academic Press, New York, **1997**, pp. 307.
[21] R. Hooft, *COLLECT Data collection Software*, Nobius B. V., Delft, The Netherlands, **1998**.
[22] A. Altomare, M. C. Burla, M. Camalli, G. L. Cascarano, C. Giacovazzo, A. Guagliardi, A. G. G. Moliterni, G. Polidori, R. Spagna, *J. Appl. Crystallogr.* **1994**, *27*, 435.
[23] G. M. Sheldrick, *SHELXL-97*. Program for crystal structure analysis, Vol. release 97-2, University of Göttingen, Germany, **1997**.
[24] L. J. Farrugia, *J. Appl. Crystallogr.* **1997**, *30*, 565.
[25] A. D. Becke, *J. Chem. Phys.* **1992**, *96*, 215.
[26] A. D. Becke, *J. Chem. Phys.* **1993**, *98*, 5648.
[27] C. Lee, W. Yang, R. G. Parr, *Phys. Rev. B* **1998**, *B37*, 785.
[28] D. Andrae, U. Haussermann, M. Dolg, H. Stoll, H. Preuss, *Theor. Chim. Acta* **1990**, *77*, 123.
[29] N. Golbout, D. R. Salahub, J. Andzelm, E. Winner, *Can. J. Chem.* **1992**, *70*, 560.
[30] P. J. Hay, W. R. Wadt, *J. Chem. Phys.* **1985**, *82*, 299.
[31] P. J. Hay, W. R. Wadt, *J. Chem. Phys.* **1985**, *82*, 284.
[32] P. J. Hay, W. R. Wadt, *J. Chem. Phys.* **1985**, *82*, 270.
[33] J. B. Nicholas, *Top. Catal.* **1997**, *4*, 157.
[34] L. A. Curtis, K. Raghavachari, P. C. Redfern, J. A. Pople, *Chem. Phys. Lett.* **1997**, *270*, 419.
[35] D. M. Smith, B. T. Golding, L. Radom, *J. Am. Chem. Soc.* **1999**, *121*, 9388.
[36] A. K. Chandra, M. T. Nguyen, *Chem. Phys* **1998**, *232*, 299.
[37] J. B. Nicholas, *Top. Catal.* **1999**, *9*, 181.
[38] R. Arnaud, C. Adamo, M. Cossi, A. Millet, Y. Valle, V. Barone, *J. Am. Chem. Soc.* **2000**, *122*, 324.
[39] H. B. Schlegel, *J. Comput. Chem.* **1982**, *3*, 214.
[40] M. J. Frisch, G. W. Trucks, H. B. Schlegel, G. E. Scusseria, M. A. Robb, J. R. Cheeseman, V. G. Zakrzewski, J. A. Montgomery, T. Vreven, K. N. Kudin, J. C. Burant, J. M. Millan, S. S. Iyengar, J. Tomasi, V. Barone, B. Mennucci, M. Cossi, G. Scalmani, N. Rega, G. A. Petersson, H. Nakatsuji, M. Hada, M. Ehara, K. Toyota, F. R., J. Hasegawa, M. Ishida, T. Nakajima, Y. Honda, O. Kitao, H. Nakai, M. Klene, X. Li, J. E. Knox, H. P. Hratchian, J. B. Cross, C. Adamo, J. Jaramillo, R. Gomperts, R. E. Stratmann, O. Yazyev, A. J. Austin, R. Cammi, C. Pomelli, J. W. Ochterski, P. Y. Ayala, K. Morokuma, G. A. Voth, P. Salvador, J. J. Dannenberg, V. G. Zakrzewski, S. Dapprich, A. D. Daniels, M. C. Strain, O. Farkas, D. K. Malick, A. D. Rabuck, K. Raghavachari, J. B. Foresman, J. V. Ortiz, Q. Cui, A. G. Baboul, S. Clifford, J. Cioslowski, B. B. Stefanov, G. Liu, A. Liashenko, P. Piskorz, I. Komaromi, R. L. Martin, D. J. Fox, T. Keith, M. A. Al-Laham, C. Y. Peng, A. Nanayakkara, M. Challacombe, P. M. W. Gill, B. Johnson, W. Chen, M. W. Wong, C. Gonzalez, J. A. Pople, *Gaussian 03, Revision B.02*, Gaussian, Inc., Pittsburgh PA, **2003**.
[41] *ChemOffice 97*, Scientific Computing, Inc., Massachusetts Ave., Suite 41, Cambridge, MA 02139875, USA.

Received October 4, 2004

